Structural Chemistry (2019) 30:2181–2189
https://doi.org/10.1007/s11224-019-01407-9

ORIGINAL RESEARCH

Topological analysis of the electron localisation function (ELF) applied to the electronic structure of oxaziridine: the nature of N-O bond

Michal Michalski[1] · Agnieszka J. Gordon[1] · Slawomir Berski[1]

Received: 7 March 2019 / Accepted: 25 July 2019 / Published online: 20 August 2019

Abstract
Topological analysis of the electron localisation function (ELF), natural bond orbital and Wiberg bond index calculations have been applied to study the electronic structure of the oxaziridine molecule with a special focus on the nitrogen-oxygen bond. The calculations have been performed at the DFT(B3LYP, CAM-B3LYP, ωB97XD, M06-L, M06-2X) and post-Hartree-Fock (CCSD(T) and CASSCF) computational levels with applied aug-cc-pVTZ basis set. Nature of N-O bonding has been characterised by two resonance forms, N^+O^- and N^-O^+, owing to a very small population (< 0.60e) of the bonding basin V(N,O), localised in the ELF field for the N-O region. The importance of electron correlation effects for the description of the N-O bonding has been observed in the CASSCF calculations. The orbital description (Wiberg, NBO) differs from topological characterisation, indicating a single N-O bond.

Keywords N-O · Chemical bond · Single bond · Electron localisation function · ELF · Topology

Introduction

Oxaziridine, $H_2CN(H)O$, is an unstable molecule with triangular heterocycle, containing carbon, oxygen and nitrogen (see Fig. 1). Due to high electronegativity of oxygen and nitrogen, three-membered ring is relatively weak and therefore can break easily [1]. In nucleophilic substitution with small steric bulk, a nucleophile tends to attack nitrogen first, leading to ring opening. Otherwise, nucleophile attack takes place at the oxygen atom instead [2]. Most of the research was performed for oxaziridine intermediate or its derivatives due to its unstable nature [3, 4]. First oxaziridine derivatives were reported by Emmons [5]. Weak N-O bond can lead to oxygen and nitrogen substitution in many chemical reactions, such as formation of stereospecific α-hydroxyketones [6–8]. Industrial production of hydrazine is also performed through imine oxidation with hydrogen peroxide to oxaziridine [9]. Chemical properties of oxaziridine are mostly related to the N-O bond; thus, understanding of its nature is crucial for studying physical properties of the molecule.

Analysis of the nitrogen-oxygen bond lengths carried out for 2802 cyclic molecules deposited in the Cambridge Structural Database, CSD [10], and presented at the histogram in Fig. 2 reveals that the majority of the N-O contacts are between 1.43 and 1.45 Å (27.9%) and 1.41 and 1.43 Å (27.6%). The N-O bond lengths in oxaziridine derivatives are between 1.48 and 1.53 Å; thus, they are longer than average N-O bonds in the solid state. For atypically long N-O bond, an interesting electronic structure is expected.

Oxaziridine molecule has been previously investigated by Taghizadeh et al. [11], who applied Fukui functions [12] and studied the topography of molecular electrostatic potential, MEP, at the DFT(B3LYP)/6-311++G(d,p) level. Calculated Fukui functions show a carbon atom as possible site for electrophilic or nucleophilic attack. According to the MEP analysis, negative charges can be found on the O and N atoms and positive charges are present on the H atoms.

In our previous papers, the nature of formally single nitrogen-oxygen bond has been investigated using topological analysis of electron localisation function, η(r) (ELF), in small XONO (X = H, F, Cl, Br, I, OH, $(CF_3)N$, Li, Na, K, Rb, CH_3, C_2H_5) molecules [13]. Our calculations showed that the

✉ Slawomir Berski
slawomir.berski@chem.uni.wroc.pl

[1] Faculty of Chemistry, University of Wroclaw, 14 F. Joliot-Curie, 50-383 Wroclaw, Poland

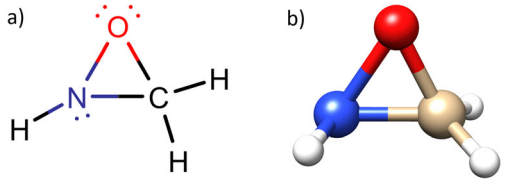

Fig. 1 **a** The Lewis formula for the oxaziridine molecule. **b** CCSD(T)/aug-cc-pVTZ optimised structure of the oxaziridine molecule

population of formally single bond N-O differs essentially from 2e expected for a single N-O bond and its value lies between 0.24e and 0.57e. Furthermore, its electron density is highly delocalised. Thus, the nature of the bond is not based on an electron pair sharing by two atoms but stems from electron density fluctuation between the N and O atoms. Despite the large amount of knowledge about the N-O bonding, it must be emphasised that the nature of the N-O bond in a cycled molecule has not yet been studied using topological approach.

The main focus of this paper is a detailed analysis — using the DFT and post-Hartree-Fock methods, (CCSD(T), CASSCF) — of the chemical bonding nature of oxaziridine, where the N-O bond is contained in the triatomic cycled molecule. Our methods of the choice are topological analysis of η(r), electron density, ρ(r), and natural bonding orbitals (NBO) theory. Overall, the study expands knowledge about non-typical covalent bonds.

Computational details

Geometry optimisations have been performed in the gas phase, 0 K, with the Gaussian09 (G09) programme (version E.01) [14] using B3LYP [15–18], CAM-B3LYP [19], ωB97XD [20], M06-L [21] and M06-2X [22] electron density functionals as included in G09. The aug-cc-pVTZ basis set [23, 24], used for all the calculations, has been downloaded from the EMSL Basis Set Library [25, 26]. Each minimum on the potential energy surface has been confirmed by harmonic frequency analysis with no imaginary frequencies. For the DFT results, each optimised structure has been additionally confirmed by a stability test (stable keyword in G09).

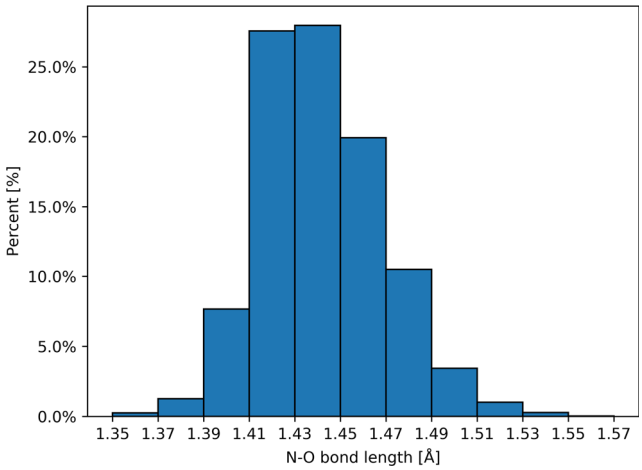

Fig. 2 Histogram of the N-O bond lengths for cyclic molecules with formally single nitrogen-oxygen bond in the ring, deposited in the Cambridge Structural Database

Optimised CCSD(T) [27, 28] structure has been taken as an initial geometry for the CASSCF(N,M) (complete active space self-consistent field) calculations: CASSCF(6,6), CASSCF(8,8) and CASSCF(10,10). First of all, the CASSCF calculations have been carried out with six electrons on the three occupied and three unoccupied orbitals (MOs), HOMO-2 to LUMO+2. Subsequently, the active space has been increased by adding one occupied molecular orbital and one virtual orbital, HOMO-3 to LUMO+3. Finally, the active space has been increased with 10 electrons on five occupied MOs, HOMO-4 to HOMO, and five unoccupied MOs, LUMO to LUMO+4.

Analysis of natural bond orbitals [29] has been carried out with the NBO 3.1 procedure available in the G09 programme.

Wave functions for topological analysis of ρ(r) and η(r) fields have been approximated using a set of MOs from single point energy calculations, performed using optimised structures (NoSymm keyword). For the CCSD(T) — optimised structures, wave functions have been calculated at the CCSD level (CCSD/aug-cc-pVTZ//CCSD(T)/aug-cc-pVTZ) using the approximation proposed by Feixas et al. [30] with the natural orbitals and their occupancies only. Similar procedure has been applied for the CASSCF data.

Topological analysis of ρ(r) and η(r) has been performed using TopMod09 package [31] and DGrid 5.0 [32] programme. Electron localisation functions have been calculated with a cubical grid with step size of 0.05 bohr. Analysis of molecular orbital (MO) contribution to the ELF and electron localizability indicator (ELI-D) has been performed using DGrid 5.0.

Graphical representations of ELF and MO have been visualised in the Multiwfn [33] and Chimera [34] programmes.

Results and discussion

Geometrical structure

Bond lengths for the optimised geometrical structure of the oxaziridine molecule (see Fig. 1), calculated using DFT(B3LYP, CAM-B3LYP, ωB97XD, M06-L, M06-2X) methods and post-Hartree-Fock techniques: the couple-cluster CCSD(T) and CASSCF with the aug-cc-pVTZ basis set, are presented in Table 1.

Application of ab initio methods with explicit electron correlation (CCSD(T), CASSCF) yields the C-O, C-N and N-O bonds longer than those obtained using the DFT methods. The

Table 1 The bond length, r, partial atom charges calculated by the AIM method, q_{AIM}, delocalisation indices, DI, and properties of the bond critical point for the N-O bond

Functional	r(N,O) (Å)			q_{AIM} (e)			DI			(3,−1) CP point for N-O bond		
	C-O	C-N	N-O	C	N	O	C-O	C-N	N-O	$\rho_{(3,-1)}(r)$ (e/au^3)	$\nabla^2\rho_{(3,-1)}(r)$ (e/au^5)	R_{BCP}/R_{eq}
B3LYP	1.397	1.434	1.495	+0.70	−0.50	−0.66	0.89	0.93	1.21	0.245	0.144	0.471
CAM-B3LYP	1.391	1.426	1.474	+0.70	−0.52	−0.68	0.88	0.93	1.22	0.258	0.094	0.474
M06-2X	1.387	1.430	1.463	+0.74	−0.52	−0.70	0.87	0.92	1.23	0.266	0.073	0.473
M06-L	1.382	1.430	1.475	+0.78	−0.49	−0.69	0.87	0.92	1.23	0.262	0.080	0.473
ωB97XD	1.388	1.427	1.470	+0.73	−0.52	−0.69	0.87	0.93	1.23	0.262	0.081	0.473
CCSD [1)]	1.401	1.442	1.509	+0.73	−0.53	−0.70	0.77	0.85	1.21	0.239	0.145	0.476
CASSCF(6,6)	1.410	1.445	1.522	+0.80	−0.57	−0.70	0.81	0.89	1.20	0.233	0.150	0.478
CASSCF(8,8)	1.408	1.445	1.516	+0.79	−0.57	−0.71	0.81	0.89	1.21	0.236	0.134	0.476
CASSCF(10,10)	1.407	1.446	1.518	+0.78	−0.57	−0.70	0.82	0.89	1.21	0.235	0.136	0.476

[1] Optimisation performed using the CCSD(T)/aug-cc-pVTZ method

$\rho_{(3,-1)}(r)$, value of electron density; $\nabla^2\rho_{(3,-1)}(r)$, Laplacian of electron density; R_{BCP}/R_{eq}, ratio of the distance from BCP to the less electronegative atom

value of r(N,O), calculated at the DFT level, varies from 1.463 to 1.495 Å depending on the density functional used. The post-Hartree-Fock method, CCSD(T), yields 1.509 Å, whilst the bond length calculated using CASSCF(6,6) is 1.522 Å. Expansion of the active space (see Computational details) leads to shortening of the N-O bond to 1.516–1.518 Å. In summary, the N-O bond length varies from 1.463 to 1.522 Å, depending on the level of calculation and falls into a typical range of N-O interaction (1.35–1.55 Å). On the other hand, setting the r(N,O) at 1.518 Å as obtained with CASSCF(10,10), and comparing to the distribution of r(N,O) lengths shown in Fig. 2 leads to a relatively long N-O bond in oxaziridine.

Local geometry of the H-N, O-N and C-N bonds corresponds to pyramidal arrangement of the bonds, thus the lone electron pair is expected to be present in the vicinity of the N atom (sp^3 hybridised). Similarly, two lone pairs should be found in the vicinity of the O atom (sp^3 hybridised). The presence of lone pairs, as predicted by the Lewis formula (see Fig. 1a), should also be supported by topological analysis of ELF.

Analysis of bonding nature

Two modern methods for investigating electronic structure of molecules, free from arbitrary choice of molecular orbitals used in this study, are topological analysis of electron density by Bader (AIM) [35] and topological analysis of ELF [36] proposed by Silvi and Savin [37]. Both methods belong to the quantum chemical topology (QCT) [38]. An electronic structure of a molecule described by ELF is represented by maxima (attractors) and its localisation basin of η(r) field, which characterise covalent bonds, lone pairs, core regions, and valence shells in atoms. Calculated electron populations on chemical bonds, $\overline{N}$, is related to integration electron density over localisation basins. Results represent average values with quantum uncertainty [39].

Firstly, the electronic structure of the $H_2CN(H)O$ molecule is investigated from the perspective of topological analysis of ρ(r) field. There are 13 critical points of ρ(r) field: six nuclear critical points (NCPs) (3,-3), six bond critical points (BCPs) (3,-1) and one ring critical point (RCP) (3,+1) in the C-N-O ring. For the N-O bond, the BCP exhibits high value of the electron density (0.233–0.266 e/au^3) and a small positive value of Laplacian of electron density, $\nabla^2\rho_{(3,-1)}(r)$, (0.073–0.150 e/au^5). Interestingly, a typical topological signature for the covalent (shared-electron) bonding is not observed, since the positive sign of $\nabla^2\rho_{(3,-1)}(r)$ suggests depletion rather than concentration of the electron density around BCP. Thus, the N-O bond, although formally single, has more complicated electronic structure than that expected using classical approach. The atomic charges calculated by the AIM method, q_{AIM}, range between 0.70e and 0.80e for the carbon atom and are significantly larger than obtained for the nitrogen (−0.57e to −0.49e) and the oxygen (−0.71e to −0.66e) atoms.

In the second step, topographical analysis has been carried out for ELF. The 2D map of η(r) function for the molecular plane defined by the C, N and O atoms (CCSD//CCSD(T) data) is presented in Fig. 3. The core regions are characterised by circular localisation domains with high (≈ 1) values of electron localisation (red), whilst the chemical bonds C-N and C-O are described by irregular localisation domains (orange) with smaller values of electron localisation (0.8–0.9). Thus, both bonds have a covalent character and exhibit high electron localisation, typical for shared electron (covalent) bonding. For the N-O bonding, a quantitatively different topography is observed since a respective

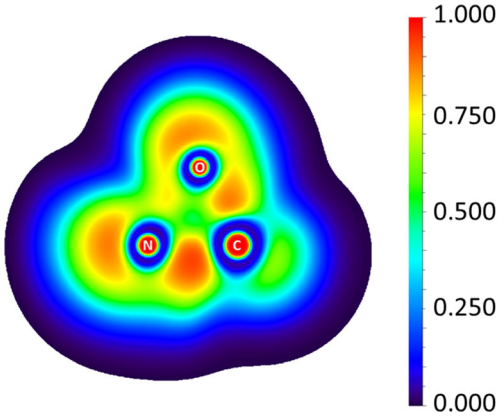

Fig. 3 The 2D map of η(r) function for the molecular plane defined by the C, N and O atoms. The ELF has been calculated using the CCSD/aug-cc-pVTZ//CCSD(T)/aug-cc-pVTZ data

localisation domain is very small, with relatively small values of ELF (0.7–0.8). The N-O bond does not show typical features of shared-electron bonding. A clear difference between the covalent C-N and C-O bonds and untypical nature of the N-O bond is evident. Such result corresponds partially with unusual (positive) values of $\nabla^2\rho_{(3,-1)}(r)$, obtained from the topological analysis of ρ(r). Further analysis of 2D map shows localisation domains corresponding to the regions of non-bonding electron density in the vicinity of the N and O atoms. Such result supports the concept of lone pairs inferred from the Lewis structure.

The delocalisation index (see Table 1), DI, is a quantitative measure of the number of electron pairs, delocalised between two atomic basins and can be used as a topological bond order [40]. The DFT and post-Hartree-Fock methods yield similar DI values. The values of DI for C-O and C-N bonds range respectively 0.77 (CCSD) – 0.89 (B3LYP) and 0.85 (CCSD) – 0.93 (B3LYP, CAM-B3LYP, ωB97XD) and suggest a typical single bond. The DI obtained for N-O bond are higher than for C-O and C-N and range between 1.20 (CASSCF(6,6)) and 1.23 (M06-2X, M06-L and ωB97XD). Thus, N-O bond exhibits a single character.

To get further insight into the electronic structure of the oxaziridine molecule, the gradient field analysis (topological analysis) has been performed for the ELF using the data obtained from the DFT and post-Hartree-Fock calculations. As a result, the core and valence attractors (local maxima), representing atomic cores, chemical bonds and lone pairs, have been found. The reader is encouraged to familiarise themselves with the publications of Silvi et al., where the principles of topological analysis of ELF are described [41–44].

Electron density of atomic cores is characterised by the C(C), C(N) and C(O) core attractors. Calculations performed using all the methods, with exception of DFT(M06-L) and DFT(B3LYP), show that the chemical bonds are represented by the V(H1,N), V(H2,C), V(H3,C), V(C,O), V(C,N) and V(N,O) attractors. Those attractors belong to the point, valence, disynaptic and bonding type, respectively. The concept of synapticity has been described by Silvi et al. in ref. [45].

The V(C,N) bonding attractor is localised approximately around the midpoint of the C-N bond, whilst the V(C,O) and V(N,O) attractors are found in the proximity of more electronegative oxygen atom. Such effect is especially visible for the N-O bond. Furthermore, the attractors are not found on an imaginary straight line linking the atomic nuclei. Such topology of ELF seems to be associated with the Pauli repulsion involved in three bonds forming a non-triangular structure. The different positions of the bonding attractors have been reported for some strained molecules (cyclopropane, cyclobutane, cyclopentane, cyclohexane, bicyclo[1.1.0]butane, spiropentane, tetrahedrane and cubane) by Chevreau and Sevin [46] and also for cyclobutane and perfluorinated cyclobutane molecules by one of us [47]. Thus, oxaziridine has more complicated structure than expected. Localisation of the V(C,O), V(C,N) and V(N,O) bonding attractors, according to the interpretation proposed by Silvi and Savin [37], clearly supports, at least partially, covalent nature of the C-O, C-N and N-O bonds. All core and valence attractors are shown in Fig. 4a.

Interestingly, for the DFT(B3LYP)/aug-cc-pVTZ and DFT(M06-L)/aug-cc-pVTZ calculations, the disynaptic bonding basin V(N,O) has not been observed. According to the interpretation by Silvi and Savin [37], this would mean that a covalent bond N-O does not exist and such a result can be associated with longest N-O bonds, obtained with both functionals (1.495 Å: B3LYP, 1.475 Å: M06-L). Electron density between the N and O atoms is characterised by the V(N,O) attractor, localised in a position where one of the oxygen's lone pair is expected (see Fig. 4b).

The protonated attractors V(H1,N), V(H2,C) and V(H3,C) are localised on hydrogens. Finally, the lone pairs on the O

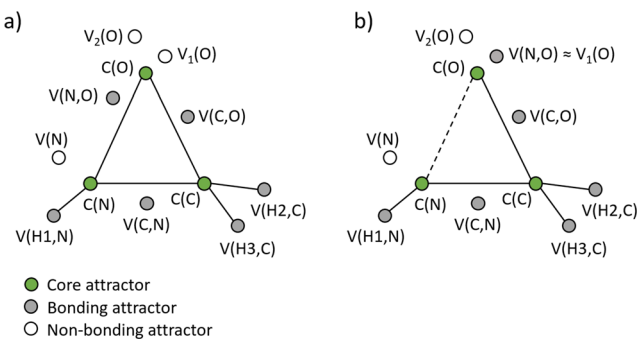

Fig. 4 **a** The core and valence attractors of ELF for the oxaziridine molecule obtained using DFT(CAM-B3LYP, ωB97XD, M06-2X), CCSD and CASSCF methods. **b** The core and valence attractors of ELF for the oxaziridine molecule obtained using B3LYP and M06-L electron density functionals. The V(N,O) attractor is localised in the point where the lone pair of the oxygen atom is expected. The analysis of atomic contributions for the V(N,O) basin shows that the basin is formed in 93% by the electron density from the O atom

and N atoms, as suggested by the Lewis formula, are confirmed by monosynaptic non-bonding attractors $V_1(O)$, $V_2(O)$ and V(N) of the point type (see Fig. 4a and b).

A difference between the N-O and other bonds is also visible, when analysing the values of ELF related to the bonding attractors. The V(N,O) is localised (M06-2X) for 0.755, much smaller value than that obtained for the most perfect electron localisation in the K-shell (1.0) and much smaller than that calculated for other bonding attractors V(H,C), V(H,N) — 1.000; V(C,N) — 0.911; and V(C,O) — 0.855. Such results suggest relatively large degree of electron delocalisation for the N-O bonding region.

The synapticity of V(N,O), the same for attractor and its basin, is presented in Fig. 5 (2D slice), where dark orange area corresponds to the disynaptic V(N,O) localisation basin. The disynaptic type is clearly visible, note that the V(N,O) basin is in contact with the core basins (blue) of nitrogen and oxygen, C(N) and C(O). The other large area corresponds to oxygen lone pairs represented by the monosynaptic, $V_1(O)$ and $V_2(O)$ basins. Their monosynaptic character is exhibited by common surfaces only with single core basin C(O). In the proximity of C(N) core basin, two large areas corresponding to the monosynaptic basin V(N) and disynaptic basin V(H1,N) are found.

To aid the interpretation of bonding character in oxaziridine, the population analysis has been carried out for the localisation basins. The basin populations, $\overline{N}$, calculated at all the computational levels, have been collected in Table 2.

Population for the N-O bond varies from 0.24e (CASSCF and CCSD) to 0.57e (M06-2X). It is worth emphasising that obtained $\overline{N}$ values are much smaller than 2e expected for the covalent single bond and even smaller than 1e. Thus, it is evident that the nature of the bonding between the N and O atoms differs quite significantly from a typical covalent bond with shared 2 electrons. In order to reflect such small basin populations, at least three resonance structures should be used, N-O, N^+O^- and N^-O^+, with dominant ionic structures, N^+O^- and N^-O^+. A small amount of electron density is not shared by the N and O atoms, but is fluctuating between the atoms. For the B3LYP and M06-L results, yielding the V(N,O) basin, characterising both the bonding and non-bonding regions and localised in the position of the oxygen lone pair, the $\overline{N}$ value for V(O) is very large, 3.22e (B3LYP) and 3.25e (M06-L). Such values are understandable since the lone pairs $V_1(O)$ and $V_2(O)$ have populations between 2.69e (CAM-B3LYP and ωB97XD) and 2.96e (CASSCF).

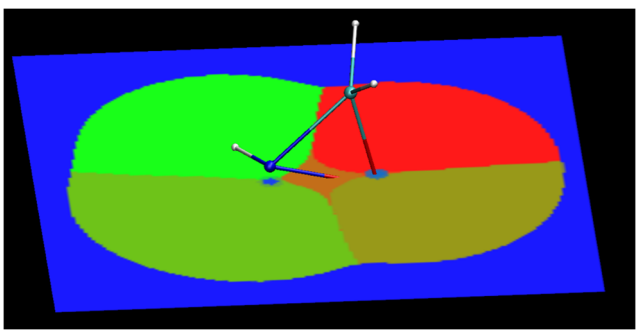

Fig. 5 The localisation basins in the oxaziridine molecule presented at 2D slice, using the CCSD/aug-cc-pVTZ//CCSD(T)/aug-cc-pVTZ data. The dark orange area in the region of the N-O bond corresponds to the V(N,O) basin. Note that the disynaptic V(N,O) basin is in contact with two core basins (blue): the C(N) and C(O)

The C-O bond has the basin population smaller than 2e; thus, (at least) three resonance structures should be used C-O, C^+O^-, C^-O^+ (less probable) in order to reflect the basin populations between 1.11e (M06-L) and 1.17e (CASSCF). The bond can be characterised by a mixture of the covalent and polar contributions. For the C-N bond, the basin populations are between 1.61e (M06-L) and 1.70e (CCSD and CASSCF). The bond can be described as a single covalent bond with some ionic character, although ionic form contribution is smaller than for the C-O bond. Some missing electron density in the C-O and N-O bonds — when comparing obtained values with formally expected value of 2e — is mainly found in the lone pair region with basin populations larger than 2e.

Populations obtained for the H-N and H-C bonds are between 2.02e and 2.06e, and between 2.09e and 2.14e. The results are in a reasonable agreement with those predicted using the Lewis formula for single bonds.

A very small basin population of the N-O bond is associated with very high delocalisation of electron density for the V(N,O) basin. The standard deviations, σ, of the basin population are 0.46 (post-Hartree-Fock) and 0.68 (DFT). High values of the σ confirm the mechanism of a fluctuating electron density in the bond. Such a result supports our conclusion that the nature of the nitrogen-oxygen interaction should be described by two resonance structures, N^+O^- and N^-O^+, rather than a single bonding pair, N-O. This mechanism is characteristic for the charge-shift (CS) model of chemical bonding, proposed by Shaik et al. [48]. However, the N-O bond classification as the CS bond is not straightforward, judging by topological analysis of electron density for heteronuclear bonds presented by Zhang et al. [49]. Positive values of $\nabla^2\rho_{(3,-1)}(r)$ between 0.073 and 0.150 e/au^5, and a large R_{BCP}/R_{eq} ratio of 0.47–0.48 are rather typical for covalent bonds, therefore do not fit the following criteria: large negative Laplacian, $\nabla^2\rho_{(3,-1)}(r)$, and a small R_{BCP}/R_{eq} ratio or proximity of BCP to less electronegative atom. Thus, the N-O bond cannot be easily classed as CS type.

Analysis of covariance of ELF basin population (see Table 3) yields information about delocalisation of electron density between basins and helps in interpretation on electron density distribution in the oxaziridine [50]. For the V(N,O) basin, electron density is mainly delocalised with lone pairs, localised on oxygen, $V_{i=1,2}(O)$, and covariance value ranges between −0.10 to −0.14, and −0.09 to −0.13, respectively. The obtained results for lone pair of nitrogen, V(N), are similar to $V_{i=1,2}(O)$ and ranges between −0.08 and −0.12. It is worth noting that delocalisation

Table 2 Values of the basin population, $\overline{N}$ (e), for the oxaziridine molecule, calculated using the wavefunction approximated using different computational methods and the aug-cc-pVTZ basis set

Basin	B3LYP	CAM-B3LYP	M06-2X	M06-L	ωB97XD	CCSD// CCSD(T)	CASSCF (6,6)	CASSCF (8,8)	CASSCF (10,10)
Core basins									
C(C)	2.09	2.09	2.09	2.09	2.09	2.09	2.09	2.09	2.09
C(N)	2.10	2.10	2.11	2.10	2.10	2.10	2.10	2.10	2.10
C(O)	2.12	2.12	2.12	2.12	2.12	2.12	2.12	2.12	2.12
Bonding basins									
V(H1,N)	2.04	2.04	2.03	2.02	2.03	2.05	2.06	2.06	2.06
V(H2,C)	2.11	2.11	2.11	2.13	2.11	2.10	2.10	2.10	2.09
V(H3,C)	2.13	2.12	2.12	2.14	2.12	2.11	2.10	2.10	2.10
V(C,O)	1.14	1.16	1.15	1.11	1.16	1.14	1.14	1.17	1.17
V(C,N)	1.66	1.66	1.64	1.61	1.65	1.68	1.70	1.70	1.70
V(N,O)	–	0.56	0.57	–	0.56	0.24	0.24	0.24	0.24
Non-bonding basins									
V_1(O)	3.22[1]	2.72	2.72	3.25[1]	2.72	2.96	2.95	2.94	2.95
V_2(O)	2.72	2.69	2.70	2.71	2.69	2.75	2.76	2.74	2.74
V(N)	2.65	2.61	2.63	2.69	2.62	2.65	2.64	2.62	2.63

[1] The V(N,O) basin also characterises the formal lone pair electron density at oxygen and the V(N,O) attractor is found in the position of V_1(O)

with electrons of the bonding V(C,N) and V(C,O) basins are smaller than obtained for lone pairs of oxygen and nitrogen atoms and equal −0.04 to −0.06 and −0.05 to −0.08, respectively.

Polarity of chemical bonds in the oxaziridine molecule has been calculated using the scheme proposed by Raub and Jansen [51], based on joined topological analysis of the ρ(r) and η(r) fields. The polarity index, p_{XY}, ranges between 0 for homopolar bonds and 1 for idealised ionic bonds. Quantum atoms are defined through topological analysis of ρ(r) field. With exception of the CASSCF and CCSD calculations, all values of atomic contributions showed in Table 3 indicate slightly larger (50–55%) contribution of oxygen electron density to the V(N,O) basin. The N-O bond is slightly polarised towards the O atom with the value of the p_{ON} index between 0

Table 3 Covariance between V(N,O) and X = $V_{i=1,2}$(O), V(N), V(C,N), V(C,O) basins, atomic contributions to the V(N,O) basin and polarity indices. The calculations performed at the DFT and post-Hartree-Fock computational level with aug-cc-pVTZ basis set

Method	cov[V(N,O),X]					Atomic contribution (e)	p_{ON}/ p_{NO}
	V_1(O)	V_2(O)	V(N)	V(C,N)	V(C,O)		
DFT(CAM-B3LYP)	−0.14	−0.13	−0.12	−0.04	−0.05	C(N) 0.28 (50%) C(O) 0.28 (50%)	0[1]
DFT(M06-2X)	−0.11	−0.10	−0.09	−0.04	−0.05	C(N) 0.28 (49%) C(O) 0.29 (51%)	0.02[1]
DFT(ωB97XD)	−0.10	−0.10	−0.08	−0.04	−0.05	C(N) 0.27 (48%) C(O) 0.29 (52%)	0.04[1]
CCSD//CCSD(T)	−0.11	−0.11	−0.09	−0.04	−0.05	C(N) 0.22 (92%) C(O) 0.02 (8%)	0.83[2]
CASSCF(6,6)	−0.10	−0.09	−0.08	−0.06	−0.08	C(N) 0.21 (88%) C(O) 0.02 (12%)	0.83[2]
CASSCF(8,8)	−0.10	−0.10	−0.08	−0.04	−0.05	C(N) 0.22 (92%) C(O) 0.02 (8%)	0.83[2]
CASSCF(10,10)	−0.10	−0.10	−0.08	−0.04	−0.05	C(N) 0.22 (92%) C(O) 0.02 (8%)	0.83[2]

p_{ON}/p_{NO} — the polarity index

[1] The p_{ON} index indicates slightly larger contribution of the O atom to the V(N,O) bonding basin

[2] The p_{NO} index indicates larger contribution of the N atom to the V(N,O) bonding basin

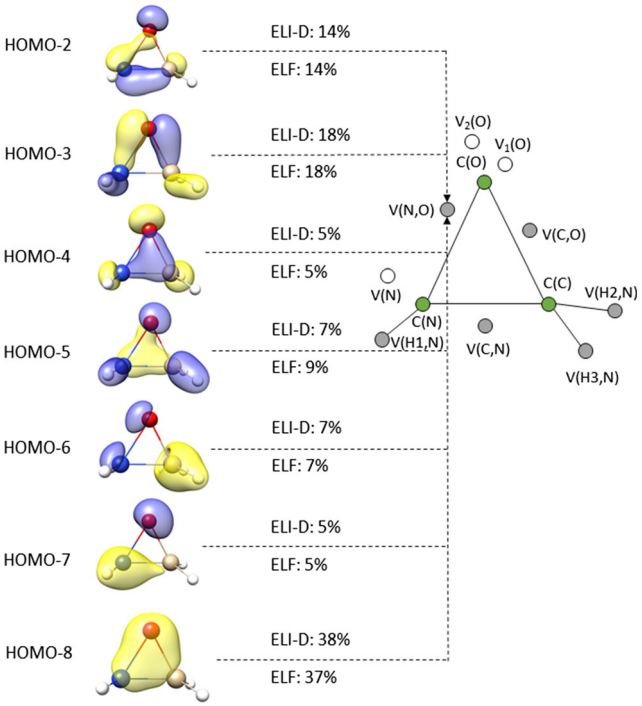

Fig. 6 Selected molecular orbitals in the oxaziridine molecule and their percentage contributions in the V(N,O) attractor of the ELI-D and ELF fields. Blue regions correspond to negative values, yellow regions to positive. Isosurfaces are plotted with value 0.13. The ELI-D and ELF have been calculated using the DFT(M06-2X)/aug-cc-pVTZ data

and 0.04. However, the CCSD and CASSCF calculation yields a very small oxygen contribution (8–12%) to the V(N,O) basin. The N-O bond is highly polarised towards the N atom with a high value of polarity index (p_{NO}), 0.83. It is worth emphasising the large difference between the p_{ON} and p_{NO} values obtained using the DFT and post-Hartree-Fock methods. In the case of the V(N,O) basin associated with the attractor localised in the unusual position, where the lone pair of the oxygen is expected (B3LYP), the atomic contributions are 0.24e (N) and 2.98e (O). Those values support our interpretation that the basin characterises mainly the non-bonding electron density of oxygen. The percentage contribution of electron density from the nitrogen is smaller than 8%. Nevertheless, the basin has common surface with two cores C(N) and C(O) and is of the disynaptic type.

Contributions of molecular orbitals (MO) to the ELF and ELI-D values [52, 53] for the V(N,O) attractor have been calculated at DFT(M06-2X)/aug-cc-pVTZ level in order to find some correlation between orbital representation of the N-O bonding and topological description using real functions. Figure 6 shows DFT-MOs with the contribution above 5%. The N-O bond is characterised by V(N,O) attractor, $\eta(r) = 0.755$, associated with contribution of the seven occupied MOs (95%). Difference between contributions to ELF and ELI-D occurs only for the two DFT-MO, HOMO-5 and the HOMO-8. However, the difference is very small (HOMO-5, 2 percentage point; HOMO-8, 1 percentage point) and can be neglected. The largest contribution to V(N,O) is from the HOMO-8 (38% by ELI-D and 37% by ELF) and the HOMO-3 (18% ELI-D and ELF). The HOMO-8 MO is localised to $\sigma_{C\text{-}O}$, $\sigma_{C\text{-}N}$ and $\sigma_{N\text{-}O}$, and generated by atomic orbitals of N, C and O atoms. The nitrogen atom has significant orbital coefficient values of 2s and three p atomic orbitals. The carbon atom contributes 2s, $2p_x$, $2p_y$ together with oxygen atom of 2s and $2p_y$ atomic orbitals. The HOMO-3 also contributes significantly to the V(N,O) attractor and is formed by the sp^2 nitrogen hybrid and overlap with the sp hybrid of oxygen atom. The HOMO-2 with 14% contribution to V(N,O) basin is generated by sp^3 hybrid of nitrogen together with sp hybrid of oxygen atom.

Additional analysis of bonding has been performed using natural bonding orbitals theory [54]. The results obtained using the DFT data are collected in Table 4. There are negative natural charges, q_{NPA}, on the nitrogen (−0.33e to −0.31e) and oxygen (−0.40e to −0.38e) atoms. However, the carbon atom has a slightly positive (0.07e – 0.08e) q_{NPA} values. Those results are in agreement with the q_{AIM} charges calculated using topological analysis of ρ(r) field. The values of the Wiberg bond order [55] for the N-O bond are close to one (1.004–1.010), indicating a single bond. Such result differs essentially from the interpretation of small (< 0.60e, DFT) and fluctuating electron density for the V(N,O) basin, with an attractor localised in the bonding region. The covalent σ-natural bond orbital, characterising N-O interaction, is formed by nitrogen and oxygen natural

Table 4 Values of the atomic charges calculated by the NPA method, q_{NPA}, Wiberg bond order and occupation for the σ-bonds for the oxaziridine molecule, calculated using a variety of electron density functionals and the aug-cc-pVTZ basis set

Functional	q_{NPA} (e)			Wiberg bond order			Occupation of σ-bond (e)		
	C	N	O	C-O	C-N	N-O	C-O	C-N	N-O
B3LYP	0.076	−0.325	−0.401	0.955	1.007	0.961	1.986	1.985	1.978
CAM-B3LYP	0.073	−0.329	−0.403	0.952	1.006	0.963	1.986	1.985	1.979
M06-2X	0.073	−0.331	−0.401	0.952	1.004	0.964	1.986	1.984	1.979
M06-L	0.082	−0.306	−0.381	0.967	1.010	0.965	1.986	1.984	1.978
ωB97XD	0.070	−0.326	−0.395	0.956	1.006	0.965	1.986	1.985	1.979

hybrid orbitals overlap with average of 9% s-orbital and 91% p-orbitals of both atoms. A larger contribution of the s-orbital can be noted for the NBOs, corresponding to the C-N and C-O bonds. The C-N has average of 21% s-orbital and 79% p-orbitals of carbon and nitrogen atoms, indicating the $sp^{3.73}$ hybrid on carbon, and also the $sp^{3.87}$ hybrid on nitrogen. Slightly smaller participation with only 2 percentage point of s-orbital in σ-bond has been found in the C-O bond, with average of 19% s-orbital and 81% p-orbitals.

The electronic structure obtained by topology analysis of ρ(r) and η(r) fields indicate that the nature of the N-O bonding is far from being single N-O bond and its description depends on the computational method used.

Conclusions

The electronic structure of the oxaziridine molecule has been investigated using topological analysis of the ELF and electron density. The current research increases our knowledge about the nature of the nitrogen-oxygen bonding in molecular systems. Furthermore, the obtained results allow to explain the unstable nature of the oxaziridine through specific nature of the N-O bond.

The nitrogen-oxygen bond is an electron-depleted bond, when compared with the classical 2e N-O bond predicted by the Lewis formula. The Wiberg bond order together with electron delocalisation obtained from AIM analysis indicate typical single N-O interaction. A small amount of electron density in the V(N,O) basin (0.24e – 0.57e), associated with the attractor localised between the N and O atoms, and a large standard deviation of the basin population indicate the fluctuating mechanism of the bonding. Thus, the nature of the N-O bond is not associated with shared electron density in the bonding region and the covalency of the N-O bond is negligible. Analysis of the results suggests that the N^+O^- and N^-O^+ representation for the nitrogen-oxygen bond instead of classical N-O formula should provide a better description of the bond nature.

Topology of the ELF for the oxaziridine molecule depends on the computational method used and is associated with the N-O bond length. Application of the DFT(B3LYP) and DFT(M06-L) methods for geometry optimisation results in a prolonged N-O bond (over 1.474 Å) and produces unreliable results, where V(N,O) attractor is not present. On the other hand, calculations performed using post-Hartree-Fock methods, CCSD(T) and CASSCF, yield much longer N-O bonds (1.509–1.522 Å) and show the bonding attractor V(N,O). Such result confirms the importance of correlation effects for the description of electronic properties of a formally single N-O bond.

Acknowledgments The authors are grateful to the Wroclaw Centre for Networking and Supercomputing for generous allocation of computer time.

Compliance with ethical standards

Conflict of interest The authors declare they have no conflict of interest.

References

1. Ricci A (2008) Amino group chemistry: from synthesis to the life sciences. Wiley-VCH, Weinheim
2. Kurti L, Czako B (2005) Strategic applications of named reactions in organic synthesis. Academic Press, San Diego
3. Couché E, Fkyerat A, Tabacchi R (2003) Asymmetric synthesis of the cis- and trans-3,4-dihydro-2,4,8-trihydroxynaphthalen-1(2H)-ones. Helv Chim Acta 86:210–221
4. Seebach D, Yoshinari T, Beck AK, Ebert MO, Castro-Alvarez A, Vilarrasa J, Reiher M (2014) How small amounts of impurities are sufficient to catalyze the interconversion of carbonyl compounds and iminium ions, or is there a metathesis through 1,3-oxazetidinium ions? Experiments, speculations, and calculations. Helv Chim Acta 97:1177–1203
5. Emmons WD (1957) The preparation and properties of oxaziranes. J Am Chem Soc 79:5739–5754
6. Davis FA, Weismiller MC (1990) Enantioselective synthesis of tertiary α-hydroxy carbonyl compounds using [(8,8-dichlorocamphoryl)sulfonyl]oxaziridine. J Organomet Chem 55:3715–3717
7. Davis FA, Sheppard AC, Chen BC, Haque MS (1990) Chemistry of oxaziridines. 14. Asymmetric oxidation of ketone enolates using enantiomerically pure (camphorylsulfonyl)oxaziridine. J Am Chem Soc 112:6679–6690
8. Davis FA, Sheppard AC (1989) Applications of oxaziridines in organic synthesis. Tetrahedron 45:5703–5742
9. Schirmann J-P, Bourdauducq P (2001) Hydrazine. Ullmann's Encycl Ind Chem
10. Groom CR, Bruno IJ, Lightfoot MP, Ward SC (2016) The Cambridge structural database. Acta Crystallogr Sect B 72:171–179 search conducted September 2018
11. Taghizadeh MT, Vatanparast M, Nasirianfar S (2015) Oxaziridine (C-CH3NO), C-CH2NO radicals and Cl, NH2 and methyl derivatives of oxaziridine; structures and quantum chemical parameters. Chem J Moldova 10:77–88
12. Yang W, Parr RG (1985) Hardness, softness, and the fukui function in the electronic theory of metals and catalysis. Proc Natl Acad Sci U S A 82:6723–6726
13. Chauvin ER, Lepetit C, Silvi B, Alikhani E (2016) Applications of topological methods in molecular chemistry. Springer International Publishing, Cham
14. Frisch MJ, Trucks GW, Schlegel HB, Scuseria GE, Robb MA, Cheeseman JR, Scalmani G, Barone V, Mennucci B, Petersson GA, Nakatsuji H, Caricato M, Li X, Hratchian HP, Izmaylov AF, Bloino J, Zheng G, Sonnenberg JL, Hada M, Ehara M, Toyota K, Fukuda R, Hasegawa J, Ishida M, Nakajima T, Honda Y, Kitao O,

Nakai H, Vreven T, Montgomery Jr JA, Peralta JE, Ogliaro F, Bearpark M, Heyd JJ, Brothers E, Kudin KN, Staroverov VN, Keith T, Kobayashi R, Normand J, Raghavachari K, Rendell A, Burant JC, Iyengar SS, Tomasi J, Cossi M, Rega N, Millam JM, Klene M, Knox JE, Cross JB, Bakken V, Adamo C, Jaramillo J, Gomperts R, Stratmann RE, Yazyev O, Austin AJ, Cammi R, Pomelli C, Ochterski JW, Martin RL, Morokuma K, Zakrzewski VG, Voth GA, Salvador P, Dannenberg JJ, Dapprich S, Daniels AD, Farkas O, Foresman JB, Ortiz JV, Cioslowski J, Fox DJ (2013) Gaussian 09, revision E.01. Gaussian, Inc., Wallingford

15. Becke AD (1993) Density-functional thermochemistry. III. The role of exact exchange. J Chem Phys 98:5648–5652
16. Lee C, Yang W, Parr RG (1988) Development of the Colle-Salvetti correlation-energy formula into a functional of the electron density. Phys Rev B 37:785–789
17. Vosko SH, Wilk L, Nusair M (1980) Accurate spin-dependent electron liquid correlation energies for local spin density calculations: a critical analysis. Can J Phys 58:1200–1211
18. Stephens PJ, Devlin FJ, Chabalowski CF, Frisch MJ (1994) Ab initio calculation of vibrational absorption and circular dichroism spectra using density functional force fields. J Phys Chem 98: 11623–11627
19. Yanai T, Tew DP, Handy NC (2004) A new hybrid exchange–correlation functional using the Coulomb-attenuating method (CAM-B3LYP). Chem Phys Lett 393:51–57
20. Chai J-D, Head-Gordon M (2008) Long-range corrected hybrid density functionals with damped atom–atom dispersion corrections. Phys Chem Chem Phys 10:6615–6620
21. Zhao Y, Truhlar DG (2006) A new local density functional for main-group thermochemistry, transition metal bonding, thermochemical kinetics, and noncovalent interactions. J Chem Phys 125:194101
22. Zhao Y, Truhlar DG (2008) The M06 suite of density functionals for main group thermochemistry, thermochemical kinetics, noncovalent interactions, excited states, and transition elements: two new functionals and systematic testing of four M06-class functionals and 12 other function. Theor Chem Accounts 120:215–241
23. Dunning TH (1989) Gaussian basis sets for use in correlated molecular calculations. I. The atoms boron through neon and hydrogen. J Chem Phys 90:1007–1023
24. Kendall RA, Dunning TH, Harrison RJ (1992) Electron affinities of the first-row atoms revisited. Systematic basis sets and wave functions. J Chem Phys 96:6796–6806
25. Schuchardt KL, Didier BT, Elsethagen T, Sun L, Gurumoorthi V, Chase J, Li J, Windus TL (2007) Basis set exchange: a community database for computational sciences. J Chem Inf Model 47:1045–1052
26. Feller D (2018) The role of databases in support of computational chemistry calculations. J Comput Chem 17:1571–1586
27. Bartlett RJ, Purvis GD (1978) Many-body perturbation theory, coupled-pair many-electron theory, and the importance of quadruple excitations for the correlation problem. Int J Quantum Chem 14: 561–581
28. Pople JA, Head-Gordon M, Raghavachari K (1987) Quadratic configuration interaction. A general technique for determining electron correlation energies. J Chem Phys 87:5968–5975
29. Glendening ED, Reed AE, Carpenter JE, Weinhold F (1998) NBO Version 3.1. TCI. University of Wisconsin, Madison
30. Feixas F, Matito E, Duran M, Solà M, Silvi B (2010) Electron localization function at the correlated level: a natural orbital formulation. J Chem Theory Comput 6:2736–2742
31. Noury S, Krokidis X, Fuster F, Silvi B (1999) Computational tools for the electron localization function topological analysis. Comput Chem 23:597–604
32. Kohout M (2017) Program DGrid, version 5.0
33. Lu T, Chen F (2011) Multiwfn: a multifunctional wavefunction analyzer. J Comput Chem 33:580–592
34. Pettersen EF, Goddard TD, Huang CC, Couch GS, Greenblatt DM, Meng EC, Ferrin TE (2004) UCSF Chimera - a visualization system for exploratory research and analysis. J Comput Chem 25:1605–1612
35. Bader RFW (1990) Atoms in molecules: a quantum theory. Oxford University Press, Oxford
36. Becke AD, Edgecombe KE (1990) A simple measure of electron localization in atomic and molecular systems. J Chem Phys 92: 5397–5403
37. Silvi B, Savin A (1994) Classification of chemical bonds based on topological analysis of electron localization functions. Nature 371: 683
38. Malcolm N, Popelier PLA (2003) The full topology of the Laplacian of the electron density: scrutinising a physical basis for the VSEPR model. Faraday Discuss 124:353–363
39. Fuentealba P, Chamorro E, Santos JC (2007) Chapter 5 understanding and using the electron localization function. Theor Comp Chem 19:57–85
40. Fradera X, Austen MA, Bader RFW (1999) The Lewis model and beyond. J Phys Chem A 103:304–314
41. Silvi B (2000) Direct space representation of the metallic bond. J Phys Chem A 104:947–953
42. Krokidis X, Noury S, Silvi B (1997) Characterization of elementary chemical processes by catastrophe theory. J Phys Chem A 101: 7277–7282
43. Alikhani ME, Fuster F, Silvi B (2005) What can tell the topological analysis of ELF on hydrogen bonding? Struct Chem 16:203–210
44. Fuster F, Silvi B (2000) Does the topological approach characterize the hydrogen bond? Theor Chem Accounts 104:13–21
45. Silvi B (2002) The synaptic order: a key concept to understand multicenter bonding. J Mol Struct 614:3–10
46. Chevreau H, Sevin A (2000) An electron localization function study of the strain energy in carbon compounds. Chem Phys Lett 322:9–14
47. Berski S, Gordon AJ, Latajka Z (2014) Electron localization function study on the chemical bonding in a real space for tetrahedrane, cubane, adamantane, and dodecahedrane and their perfluorinated derivatives and radical anions. J Phys Chem A 118:4147–4156
48. Shaik S, Danovich D, Silvi B, Lauvergnat DL, Hiberty PC (2005) Charge-shift bonding - a class of electron-pair bonds that emerges from valence bond theory and is supported by the electron localization function approach. Chem Eur J 11:6358–6371
49. Zhang L, Ying F, Wu W, Hiberty PC, Shaik S (2009) Topology of electron charge density for chemical bonds from valence bond theory: a probe of bonding types. Chem Eur J 15:2979–2989
50. Silvi B (2004) How topological partitions of the electron distributions reveal delocalisation. Phys Chem Chem Phys 6:256–260
51. Raub S, Jansen G (2001) A quantitative measure of bond polarity from the electron localization function and the theory of atoms in molecules. Theor Chem Accounts 106:223–232
52. Kohout M (2004) A measure of electron localizability. Int J Quantum Chem 97:658
53. Kohout M (2007) Bonding indicators from electron pair density functionals. Faraday Discuss 135:43–54
54. Weinhold F (1998) Encyclopedia of computational chemistry. John Wiley & Sons, Chichester
55. Wiberg KB (1966) Application of the Pople-Santry-Segal CNDO method to the cyclopropylcarbinyl and cyclobutyl cation and to bicyclobutane. Tetrahedron 24:1083–1096